



OPEN

## Oncogenic signaling inhibits c-FLIP<sub>L</sub> expression and its non-apoptotic function during ECM-detachment

Matyas Abel Tsegaye<sup>1,2</sup>, Jianping He<sup>1,3</sup>, Kyle McGeehan<sup>1</sup>, Ireland M. Murphy<sup>1</sup>,  
Mati Nemera<sup>1</sup> & Zachary T. Schafer<sup>1,2,3</sup>✉

Inhibition of programmed cell death pathways is frequently observed in cancer cells where it functions to facilitate tumor progression. However, some proteins involved in the regulation of cell death function dichotomously to both promote and inhibit cell death depending on the cellular context. As such, understanding how cell death proteins are regulated in a context-dependent fashion in cancer cells is of utmost importance. We have uncovered evidence that cellular FLICE-like Inhibitory Protein (c-FLIP), a well-known anti-apoptotic protein, is often downregulated in tumor tissue when compared to adjacent normal tissue. These data argue that c-FLIP may have activity distinct from its canonical role in antagonizing cell death. Interestingly, we have discovered that detachment from extracellular matrix (ECM) serves as a signal to elevate c-FLIP transcription and that oncogenic signaling blocks ECM-detachment-induced c-FLIP elevation. In addition, our data reveal that downregulation of c-FLIP promotes luminal filling in mammary acini and that c-FLIP overexpression in cancer cells inhibits colony formation in cells exposed to ECM-detachment. Taken together, our study reveals an unexpected, non-apoptotic role for c-FLIP during ECM-detachment and raises the possibility that c-FLIP may have context-dependent roles during tumorigenesis.

Cellular FLICE (FADD-like IL-1 $\beta$ -converting enzyme)-inhibitory protein (c-FLIP) is a member of the death effector domain (DED) family of proteins along with FADD and pro-caspase 8<sup>1</sup>. While there are multiple c-FLIP variants known to be generated by alternative splicing, each variant has two DED domains and can interact with other DED-containing proteins through DED:DED interactions. These interactions drive the best characterized function of c-FLIP: its capacity to inhibit the activation of receptor-mediated cell death pathways<sup>2</sup>. Mechanistically, this occurs primarily by preventing homodimerization and activation of pro-caspase 8 on the death-inducing signaling complex (DISC). c-FLIP can also function to block necroptosis and promote cell survival by promoting the cleavage of RIPK1 on the ripoptosome<sup>3,4</sup>. As a protein known to inhibit cell death, antagonizing this function of c-FLIP has long been considered a possible strategy to sensitize cancer cells to cell death<sup>5,6</sup>.

Relatedly, the metastasis of cancer cells to distant sites is the primary cause of mortality in cancer patients<sup>7,8</sup>. For cancer cells to grow and effectively metastasize to distant sites, they must overcome several barriers during tumor progression. One such barrier is the lack of integrin-mediated attachment to the extracellular matrix (ECM), which is critical for the survival of a variety of cell types<sup>9</sup>. The term “anoikis” was coined to describe caspase-mediated cell death caused by lack of ECM-attachment<sup>10</sup> and cancer cells often disable anoikis in order to facilitate survival during metastasis<sup>8</sup>. In addition to anoikis induction, ECM-detachment results in substantial alterations in cellular metabolism that can compromise the viability of ECM-detached cells in an anoikis-independent (or caspase-independent) fashion<sup>11–15</sup>. Oncogenic signaling cascades have been discovered to result in anoikis inhibition and fundamental changes in metabolism that in aggregate function to permit the survival of ECM-detached cancer cells<sup>16–19</sup>.

Here, we report that breast cancer cells benefit from diminished c-FLIP expression, a surprising result given the well-established anti-apoptotic function of c-FLIP. We discovered that c-FLIP is diminished in breast tumors when compared to normal breast tissue and that c-FLIP expression in breast cancer is inversely correlated with the expression of oncogenes. Furthermore, ECM-detachment functions as a signal to induce c-FLIP expression in non-cancerous mammary epithelial cells. Signal transduction emanating from activated oncogenes lowers the ECM-detachment-mediated elevation in c-FLIP expression through a mechanism dependent on PI(3)K

<sup>1</sup>Department of Biological Sciences, University of Notre Dame, 222 Galvin Life Science Center, Notre Dame, IN 46556, USA. <sup>2</sup>Integrated Biomedical Sciences Program, University of Notre Dame, Notre Dame, IN 46556, USA. <sup>3</sup>Boler-Parseghian Center for Rare & Neglected Diseases, University of Notre Dame, Notre Dame, IN 46556, USA. ✉email: zschafe1@nd.edu

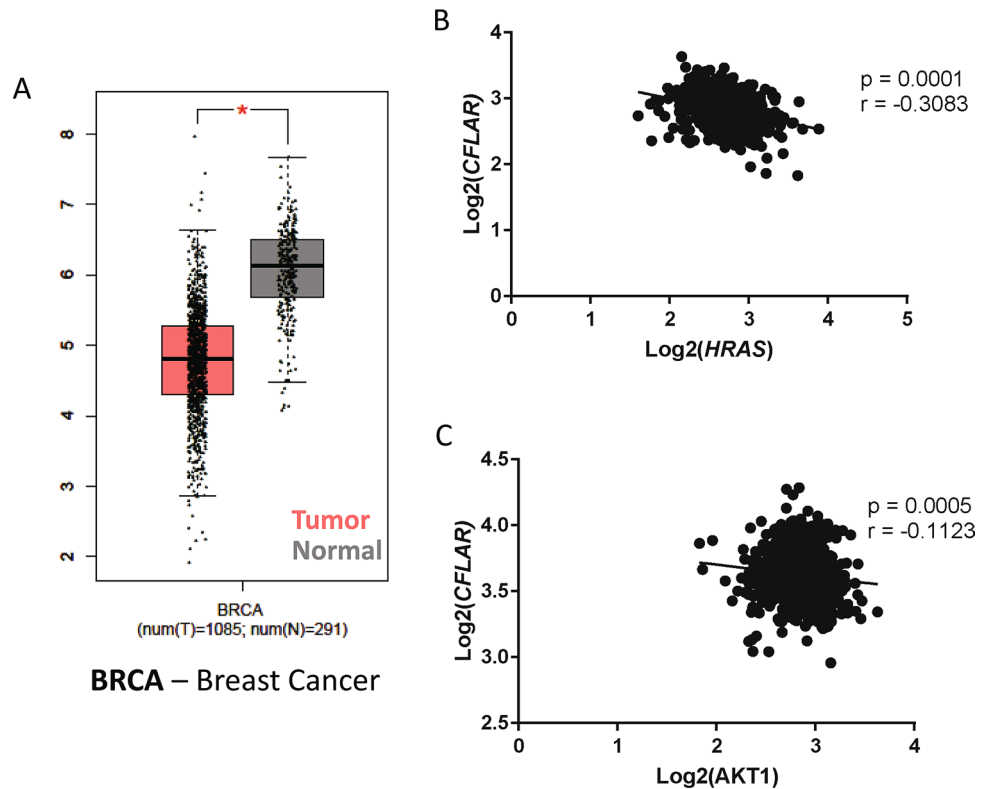


**Figure 1.** Downregulation of c-FLIP in tumors compared to normal tissue. **(A)** Comparison of *CFLAR* expression levels in tumor versus normal tissue in breast cancer samples (BRCA). **(B,C)** Correlative analysis of the expression levels of *CFLAR* with **(B)** *HRAS* and **(C)** *AKT1* in breast cancer samples. **(A)** Data was acquired using online tool known as GEPIA which utilizes TCGA (tumor and normal tissue gene expression) and GTEx (normal tissue gene expression) in order to ascertain relative expression levels of a gene across different tissues (Log<sub>2</sub>FC cutoff = 1, p value cutoff = 0.01); data is presented in Log scale.

signaling. Diminished ECM-detachment-mediated c-FLIP expression enhances luminal filling of mammary acini, and elevated c-FLIP expression can compromise the ability of breast cancer cells to grow in anchorage-independent conditions. Taken together, our data suggest a non-canonical role for c-FLIP during ECM-detachment and that downregulation of c-FLIP may have alternative functions during the course of tumorigenesis. As such, our results unveil a possible mechanism to explicate why breast tumors often have diminished c-FLIP levels and why low c-FLIP levels correlate with poor patient outcomes for breast cancer patients.

## Results

**Patient data reveal lower levels of c-FLIP in breast tumor tissue.** Given the aforementioned role of c-FLIP in blocking death receptor-mediated cell death, we reasoned that there would be elevated expression of c-FLIP in tumor tissue when compared to normal tissue. Using publicly available data to compare *CFLAR* (which encodes for c-FLIP) expression in tumors compared to normal tissue, we surprisingly observed that *CFLAR* expression was lower in breast cancer (BRCA) when compared to normal counterpart tissue (Fig. 1A). Similar findings were also observed in several other cancer types (Supplemental Fig. 1A). Given these data, we hypothesized that the downregulation in c-FLIP expression in breast tumor tissue may be a consequence of elevated oncogenic signaling. Indeed, an analysis of data derived from The Cancer Genome Atlas (TCGA) revealed an inverse correlation between the expression levels of oncogenes (*HRAS* and *AKT1*) and *CFLAR* in breast (Fig. 1B,C) and lung cancer samples (Supplemental Fig. 1B,C). Taken together, these data suggest that cancer cells benefit from lower *CFLAR* expression and may achieve this outcome as a consequence of oncogenic signaling.

**Detachment from ECM causes elevated c-FLIP expression in non-cancerous mammary epithelial cells.** Given the surprising evidence that *CFLAR* expression was diminished in breast tumors, we were interested in determining a biological rationale that could lead to such an outcome. To that end, we assessed how c-FLIP was regulated during ECM-detachment. We measured c-FLIP protein levels in established, non-cancerous mammary epithelial cell lines (MCF-10A and HMEC) and found that in both cases, ECM-detachment causes an elevation in c-FLIP protein levels (Fig. 2A). Notably, this elevation was readily apparent in the c-FLIP<sub>L</sub> isoform and that there was no evidence of detectable levels of c-FLIP<sub>S</sub> (A549 cells were used as a positive control for c-FLIP<sub>S</sub> detection). As such, we focused our subsequent studies on the regulation of c-FLIP<sub>L</sub> during ECM-

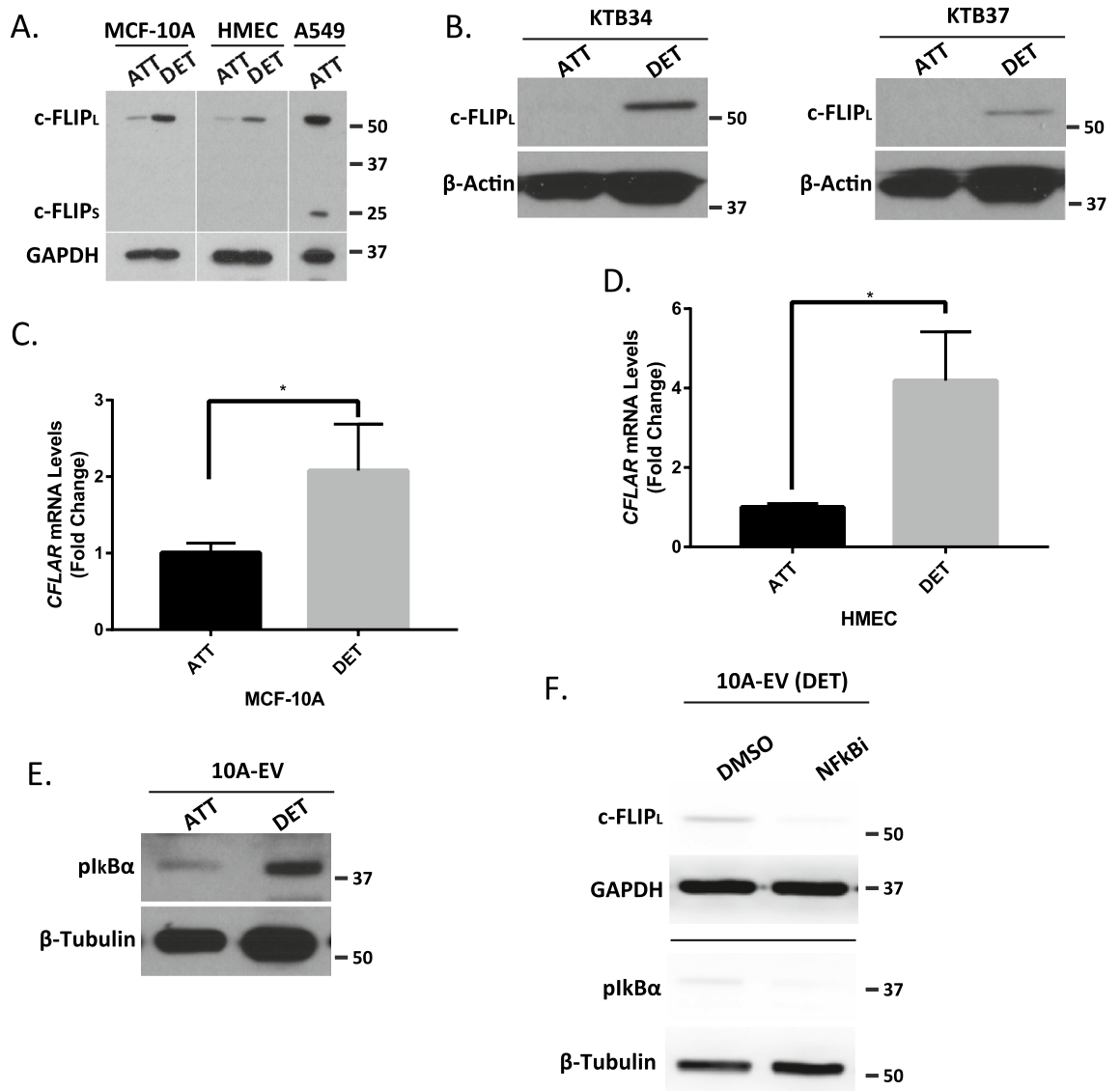


**Figure 2.** ECM-detachment triggers c-FLIP<sub>L</sub> expression in non-cancerous epithelial cells. **(A)** Measurement of c-FLIP<sub>L</sub> protein levels in MCF-10A cells in attachment (ATT) and detachment (DET) conditions using western blot. A549 cells are included as a positive control for c-FLIP<sub>S</sub>. **(B)** Measurement of c-FLIP<sub>L</sub> protein levels in KTB34 cells (left) and KTB37 cells (right) after cells were grown in attachment versus detachment conditions for 24 h. **(C,D)** Measurement of c-FLIP<sub>L</sub> transcript levels (*CFLAR*) using RT qPCR in **(C)** MCF-10A cells and **(D)** HMEC cells. **(E)** Measurement of NFκB signaling in 10A-EV cells by blotting for phospho-IκBα in attachment versus detachment conditions. **(F)** Measurement of the changes in c-FLIP<sub>L</sub> protein levels following inhibition of NFκB activity using 5 μM BAY-117082. Graphs show representative data from a minimum of three biological replicates and all western blotting experiments were independently repeated a minimum of three times with similar results. Statistical significance was determined using Student's two-tailed *t* test. Error bars show standard deviation.

detachment. In order to extend our analysis into mammary epithelial cells that more closely resemble cells found in normal mammary tissue, we measured c-FLIP<sub>L</sub> protein levels in KTB34 and KTB37 cells. These immortalized lines were derived from core biopsies of normal breast tissue and, in contrast to MCF-10A or HMEC, display either luminal A (KTB34) or normal-like (KTB37) gene expression patterns<sup>20</sup>. Much like we observed with MCF-10A or HMEC cells, ECM-detachment was a strong signal for c-FLIP<sub>L</sub> induction in KTB34 and KTB37 cells (Fig. 2B). In addition, when we assessed the capacity of ECM-detachment to alter c-FLIP<sub>L</sub> levels in a range of breast cancer lines representing distinct molecular subtypes (Supplemental Fig. 2A), the ability of ECM-detachment to cause c-FLIP<sub>L</sub> upregulation was largely not observed. Furthermore, the elevated c-FLIP<sub>L</sub> levels observed during ECM-detachment are sustained for periods of time (48 h) known to cause robust caspase activation (Supplemental Fig. 2B,C). Thus, the ECM-detachment-mediated induction in c-FLIP<sub>L</sub> does not appear to be sufficient to impact anoikis inhibition and may instead have an alternative function during ECM-detachment.

Given that levels of c-FLIP<sub>L</sub> protein have been demonstrated to be regulated by numerous mechanisms, we sought to ascertain if c-FLIP<sub>L</sub> levels were elevated during ECM-detachment as a consequence of increased *CFLAR* transcription. Indeed, we observed a robust increase in *CFLAR* transcript when MCF-10A or HMEC cells were grown in ECM-detachment (Fig. 2C,D). Notably, previous studies have revealed that NFκB signaling can function to induce the expression of c-FLIP<sub>L</sub> in various cellular contexts<sup>21</sup>. Thus, we investigated whether ECM-detachment can trigger the activation of NFκB signaling by measuring the phosphorylation of IκBα at Ser32/36, a well-known marker for NFκB activation<sup>22</sup>. Indeed, ECM-detachment resulted in robust phosphorylation of IκBα in MCF-10A cells (Fig. 2E). Furthermore, pharmacological inhibition of NFκB signaling was sufficient to block the ECM-detachment-mediated induction of c-FLIP<sub>L</sub> in cells grown in ECM-detachment (Fig. 2F). Collectively, these data suggest that loss of ECM-attachment results in transcriptional upregulation of c-FLIP<sub>L</sub> due to the activation of NFκB signaling.

**Oncogene overexpression downregulates c-FLIP<sub>L</sub> expression during ECM detachment.** Given the data suggesting that *CFLAR* expression is often downregulated in breast tumors (Fig. 1), we reasoned that the introduction of oncogenic signals in non-cancerous mammary epithelial cells may block the ECM-detachment-mediated elevation in c-FLIP<sub>L</sub>. To test this possibility, we engineered MCF-10A cells to express high levels of H-Ras (G12V), ErbB2, or EGFR (Supplemental Fig. 3A). Interestingly, overexpression of each of these oncogenes resulted in the downregulation of c-FLIP<sub>L</sub> protein in ECM-detached (but not ECM-attached) cells (Fig. 3A). Similarly, *CFLAR* expression was substantially reduced in ECM-detached cells expressing these oncogenes (Fig. 3B). Given that each of these oncogenes can promote activation of the PI(3)K/Akt pathway<sup>23</sup>, we assessed whether activation of PI(3)K or Akt is sufficient to inhibit the ECM-detachment-mediated elevation in c-FLIP<sub>L</sub>. Indeed, we observed that expression of constitutively active PI(3)K (P110α<sup>E545K</sup>) or Akt (myristoylated-Akt) resulted in reduced c-FLIP<sub>L</sub> levels in ECM-detachment (Fig. 3C, Supplemental Fig. 3B). Next, we assessed whether activation of PI(3)K-Akt is necessary to limit c-FLIP<sub>L</sub> levels in ECM-detached cells. Upon treatment with a selective inhibitor of PI(3)K, c-FLIP<sub>L</sub> protein levels were restored in ECM-detached MCF-10A cells expressing H-Ras (G12V), ErbB2, or EGFR (Fig. 3D). Similarly, treatment with the PI(3)K inhibitor restores *CFLAR* expression in MCF-10A cells engineered to have activated oncogenic signaling (Fig. 3E). However, this capacity to elevate *CFLAR* expression does not extend to control MCF-10A cells that have not been transduced with activated oncogenes (Fig. 3E).

**c-Myc is a downstream effector of PI(3)K/Akt that is associated with the downregulation of c-FLIP<sub>L</sub> expression.** Given that ECM-detachment-mediated elevation in c-FLIP<sub>L</sub> is abrogated by PI(3)K/Akt signaling, we sought to elucidate the relationship between Akt and c-FLIP<sub>L</sub>.

To do so, we first utilized a bioinformatic approach to predict relationships between *AKT1* and *CFLAR* gene expression<sup>24</sup>. This analysis revealed that c-Myc could be an intermediary linking PI(3)K/Akt activation and downregulation of *CFLAR* expression (Fig. 4A). Previous studies have discovered that c-Myc can function as a transcriptional repressor<sup>25,26</sup> and that in certain cellular contexts, c-Myc can directly repress *CFLAR* expression<sup>27</sup>. Interestingly, we found that activation of oncogenic signaling (via expression of H-Ras (G12V) or HER2) led to increased c-Myc levels in ECM-detached cells (Fig. 4B). Furthermore, this upregulation is likely due to the stabilization of c-Myc protein, as we do not detect differences in expression of *MYC* mRNA upon activation of oncogenic signaling (Fig. 4C).

One prominent and well-described regulator of the stability of c-Myc protein is GSK-3β, which phosphorylates c-Myc at threonine 58 (Thr58). This phosphorylation event is known to trigger the recruitment of E3 ubiquitin ligases and to cause proteasomal degradation of the c-Myc protein<sup>28</sup>. Furthermore, GSK-3β activity is negatively regulated by Akt-mediated phosphorylation at serine 9 (Ser9)<sup>29</sup>. As such, we reasoned that the PI(3)K-mediated downregulation of c-FLIP<sub>L</sub> during ECM-detachment may be a consequence of GSK-3β inhibition and stabilization of c-Myc protein. In support of this possibility, we observed increased phosphorylation of GSK-3β at Ser9 in cells engineered to activate oncogenic signaling (Fig. 4D). In addition, treatment of ECM-detached cells with TDZD-8, a GSK-3β inhibitor, led to elevated c-Myc protein levels (Fig. 4E) and diminished abundance of c-FLIP<sub>L</sub> (Fig. 4F). Taken together, these data support a model in which PI(3)K/Akt blocks GSK-3β activity, stabilizes c-Myc protein, and represses transcription of *CFLAR* during ECM-detachment (see model in Fig. 4G).

**c-FLIP<sub>L</sub> antagonizes the growth of ECM-detached cells.** Given the aforementioned data demonstrating that oncogenic signaling can downregulate c-FLIP<sub>L</sub> levels during ECM-detachment, we were interested in understanding if loss of c-FLIP<sub>L</sub> would confer a benefit to cells grown in ECM-detachment. As such, we utilized lentiviral delivery of shRNA to engineer MCF-10A cells to be deficient in c-FLIP<sub>L</sub> (Fig. 5A). When grown in Matrigel, MCF-10A cells will form 3-dimensional acinar structures that closely model mammary morphogenesis<sup>30</sup>. In addition, the hollowing of mammary acini is well-known to be controlled by cell death programs activated in centrally located cells that lack attachment to ECM<sup>11,14,16,31,32</sup>. Intriguingly, shRNA-mediated reduction of c-FLIP<sub>L</sub> caused a significant increase in the number of mammary acini that are scored as “mostly filled” or “filled” (Fig. 5B). Notably, we found that shRNA-mediated reduction of c-FLIP<sub>L</sub> does not appreciably alter caspase-3/7 (Supplemental Fig. 4A) or caspase-8 (Supplemental Fig. 4B) activity in ECM-detached or ECM-attached MCF-10A cells. These data suggest that the impact of shRNA-mediated reduction in c-FLIP<sub>L</sub> in MCF-10A cells is independent of alterations in caspase activation.

Given that our data suggest that loss of c-FLIP<sub>L</sub> can promote luminal filling in mammary acini, we reasoned that elevation of c-FLIP<sub>L</sub> levels in invasive breast cancer cells may compromise their capacity to thrive in an anchorage-independent setting. To test this possibility, we overexpressed c-FLIP<sub>L</sub> in MDA-MB-231 cells, a highly

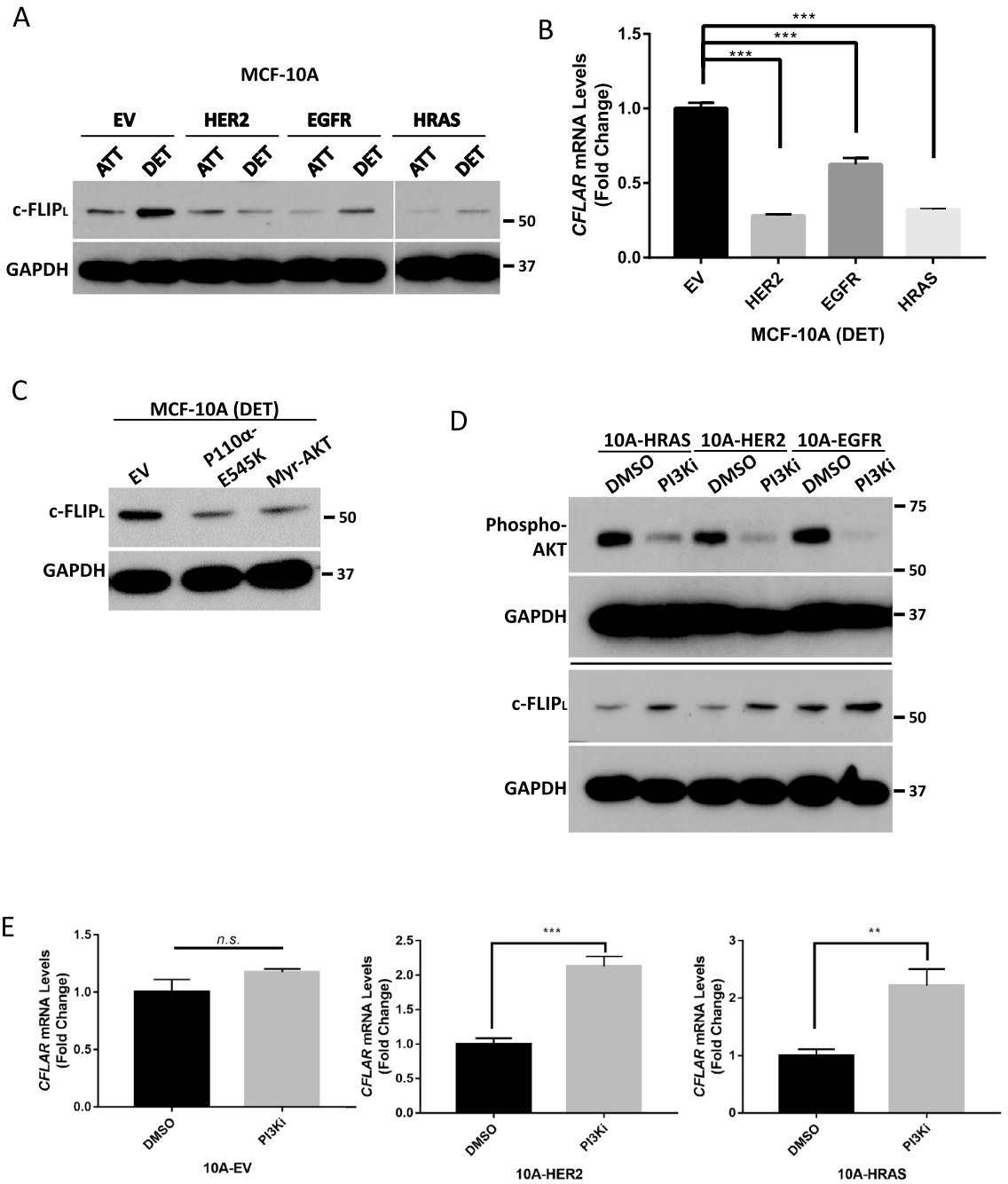


**Figure 3.** Regulation of c-FLIP<sub>L</sub> by PI(3)K/Akt signaling during ECM-detachment. (A) Measurement of c-FLIP<sub>L</sub> protein levels (in detached and attached conditions) in MCF-10A cells overexpressing oncogenes (HRAS<sup>G12V</sup>, HER2, EGFR) as compared to empty vector (EV) control. (B) RT-qPCR measurement of *CFLAR* in MCF-10A cells overexpressing oncogenes versus EV control. (C) Measurement of c-FLIP<sub>L</sub> protein levels in MCF-10A cells overexpressing oncogenes (p110α<sup>E545K</sup> and myr-AKT) as compared to EV control. (D) Measurement of c-FLIP<sub>L</sub> levels after treatment of oncogene overexpressing MCF-10A cells with small molecule inhibitor of PI3Kα, BYL719 (10 μM). (E) Measurement of *CFLAR* levels in oncogene overexpressing MCF-10A cell treated with BYL719. Graphs show representative data from a minimum of three biological replicates and all western blotting experiments were independently repeated a minimum of three times with similar results. Statistical significance was determined using Student’s two-tailed *t* test. Error bars show standard deviation. All panels show cells grown in ECM-detached conditions.

aggressive, triple negative breast cancer line (Fig. 5C). Indeed, c-FLIP<sub>L</sub> compromised the viability of these cells when grown in ECM-detached conditions (Fig. 5D). Similarly, when cells were grown in ECM-detachment and then re-plated at low density in ECM-attached conditions, c-FLIP<sub>L</sub> expression blocked the capacity of these cells

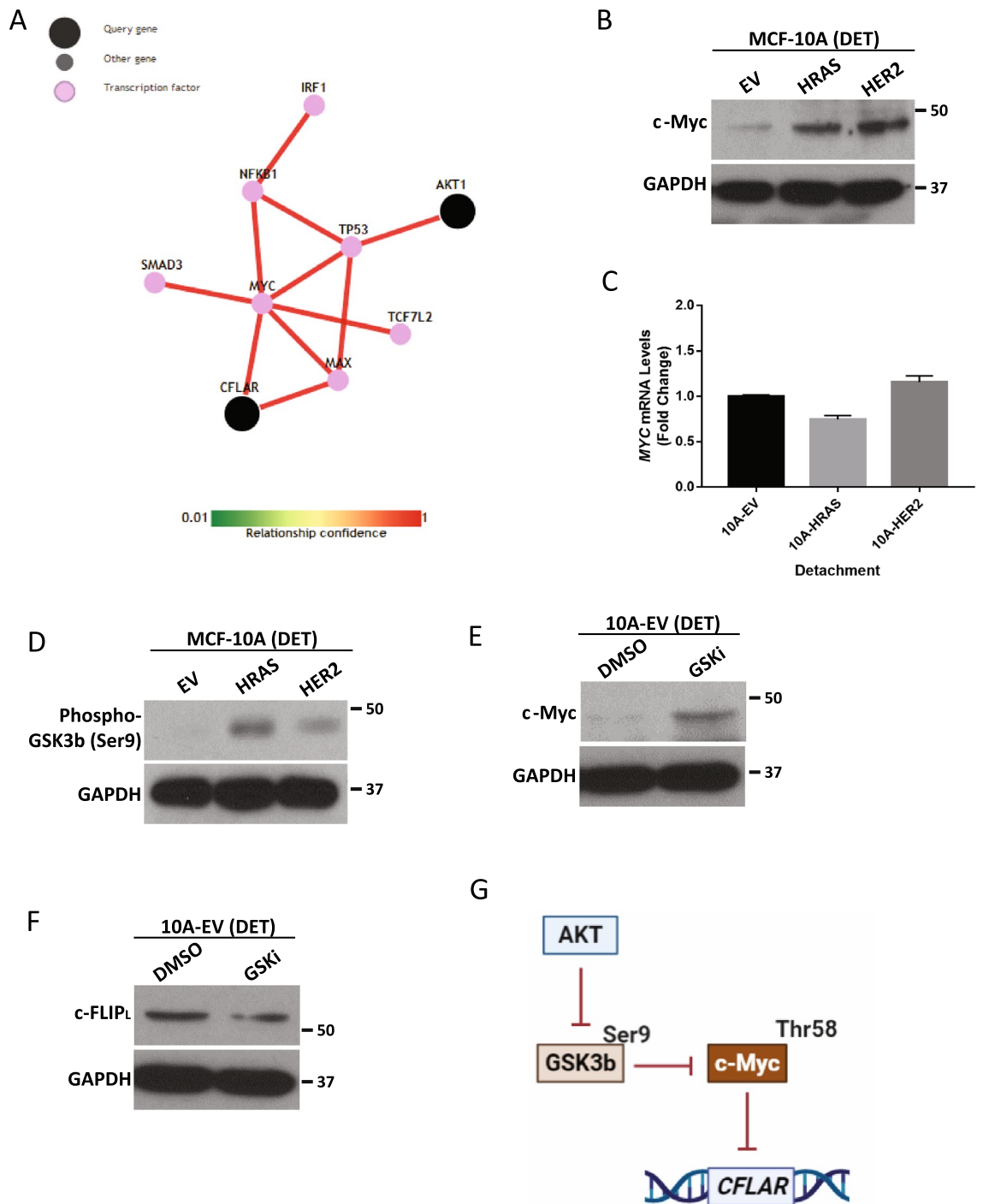


**Figure 4.** Transcriptional regulation of c-FLIP<sub>L</sub> during ECM-Detachment. (A) In-silico analysis of the transcriptional relationship between *CFLAR* and *AKT1* using a pathway prediction tool (<http://pathwaynet.princeton.edu>). (B) Measurement of c-Myc levels in oncogene overexpressing MCF-10A cells as compared to EV control. (C) Measurement of c-Myc transcript levels using RT-qPCR in oncogene overexpressing MCF-10A cells as compared to EV control. (D) Measurement of GSK-3β activity by blotting for its phosphorylation at serine 9. (E) Inhibition of GSK-3β activity using 25 μM TDZD-8 (GSK-3β inhibitor) in 10A-EV cells. (F) Determination of c-FLIP<sub>L</sub> protein levels in 10A-EV cells after the inhibition of GSK-3β activity using 25 μM TDZD-8. (G) Schematic representation of transcriptional regulation of c-FLIP<sub>L</sub> by Akt. Graphs show representative data from a minimum of three biological replicates and all western blotting experiments were independently repeated a minimum of three times with similar results. Cells were grown in ECM-detached conditions in all panels. Statistical significance was determined using Student’s two-tailed *t* test. Error bars show standard deviation.

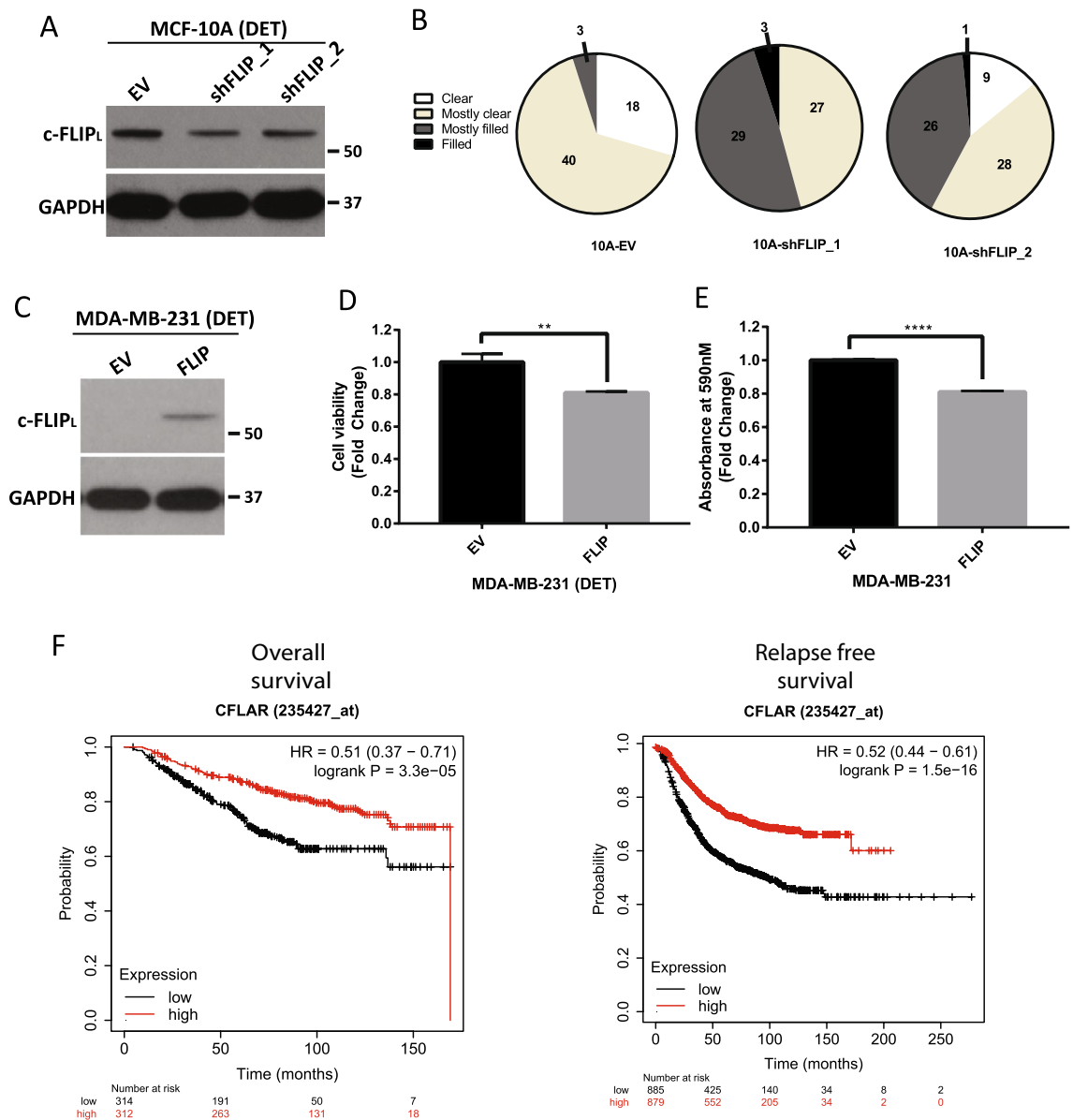


**Figure 5.** c-FLIP<sub>L</sub> negatively impacts ECM-detached cell growth. **(A)** MCF-10A cells were stably transfected with shRNA targeting c-FLIP<sub>L</sub> and efficacy was verified with western blot. **(B)** 10A-EV, 10A-shFLIP1 and 10A-shFLIP2 cells were grown in 3D Matrigel Assay and were allowed to form acinar structures for 18 days. Structures were stained and luminal clearance was scored as described. 10A-EV  $n = 61$ , 10A-shFLIP1  $n = 59$ , 10A-shFLIP2  $n = 64$ . **(C)** c-FLIP<sub>L</sub> was overexpressed in MDA-MB-231 cells and verified by western blot. **(D)** Measurement of cell viability MDA-MB-231 cells during ECM-detachment using CellTiter-Glo Luminescent Cell Viability Assay after 48 h. **(E)** Long term clonogenic assay of MDA-MB-231 cells tested as described and stained with crystal violet assay. Absorbance of extracted crystal violet at 590 nm is shown. **(F)** Correlation of c-FLIP<sub>L</sub> expression to overall survival and relapse-free survival of patients with breast cancer. c-FLIP<sub>L</sub> expression is differentiated as low (black) vs high (red) expression against the median expression. Overall survival was analyzed using KMPlotter (<http://www.kmplot.com>). Graphs show representative data from a minimum of three biological replicates and all western blotting experiments were independently repeated a minimum of three times with similar results. Statistical significance was determined using Student's two-tailed  $t$  test. Error bars show standard deviation.

to form colonies (Fig. 5E). Given the data that lower levels of c-FLIP<sub>L</sub> may facilitate the growth of ECM-detached cancer cells, we hypothesized that low levels of c-FLIP<sub>L</sub> may be associated with poor clinical outcomes owing to tumor cell dissemination. Indeed, analysis of data derived from breast cancer patients revealed that lower levels of *CFLAR* expression was linked to poor patient outcomes as measured by diminished overall survival and relapse-free survival (Fig. 5F).

## Discussion

Our findings describe an unexpected role for c-FLIP<sub>L</sub> during ECM-detachment that may account for the observed downregulation of c-FLIP<sub>L</sub> in breast cancers. Furthermore, our results demonstrate that the ECM-detachment-mediated elevation in c-FLIP<sub>L</sub> expression is counteracted by oncogenic signaling through activation of the PI(3)K/Akt pathway. Oncogenic activation of PI(3)K/Akt is associated with inhibition of GSK-3 $\beta$  and an elevation in c-Myc-mediated downregulation of *CFLAR* expression. In support of these data, we found that diminished *CFLAR* expression (which functions to facilitate the survival of ECM-detached cells) is correlated with poor clinical outcomes in breast cancer patients. As such, our studies reveal that restoration of this novel c-FLIP<sub>L</sub> activity may be an attractive chemotherapeutic strategy to eliminate ECM-detached cancer cells prior to (or during) metastatic dissemination.

Our findings raise interesting questions regarding dichotomous and context-dependent roles for c-FLIP<sub>L</sub> during the course of tumorigenesis. More specifically, there appears to be substantial evidence of downregulation of c-FLIP<sub>L</sub> in breast tumors where low c-FLIP<sub>L</sub> is also associated with oncogenic signaling and with poor patient outcomes. The ability of c-FLIP<sub>L</sub> to antagonize the ability of ECM-detached cancer cells to grow may be related to the observed changes in c-FLIP<sub>L</sub> in tumors derived from breast cancer patients. Additionally, we do have data (see Supplemental Fig. 1) that reveal some other cancers also have diminished c-FLIP<sub>L</sub> levels compared to normal tissue. Future studies aimed at broadening an assessment of c-FLIP<sub>L</sub> in tumors of distinct origins, and the relationship between oncogenic signaling and c-FLIP<sub>L</sub> in other types of cancer cells, will be important for better understanding the implications of these findings. Furthermore, any efforts to therapeutically restore c-FLIP<sub>L</sub> activity to restrict tumor progression would have to contend with the context-dependent nature of c-FLIP<sub>L</sub> activity. The capacity of c-FLIP<sub>L</sub> to block cell death by apoptosis has been thoroughly described and thus, it is important to have a better understanding of the molecular circumstances that underlie when c-FLIP<sub>L</sub> can be pro-tumorigenic compared to when c-FLIP<sub>L</sub> can be anti-tumorigenic (as may be the case during ECM-detachment).

In addition, the contrast between c-FLIP<sub>L</sub> function in ECM-detachment and in other contexts is stark. The well-characterized anti-apoptotic roles of c-FLIP<sub>L</sub> are, on the surface, difficult to reconcile with the function of c-FLIP<sub>L</sub> described in ECM-detachment. However, there are indeed other reported instances where c-FLIP<sub>L</sub> has been demonstrated to have multiple roles with regards to cell death regulation. For example, c-FLIP null mice do not survive beyond day 10.5 of embryogenesis due to defects in heart development<sup>33</sup>. This phenotype is similar to that observed of FADD<sup>-/-</sup> or caspase 8<sup>-/-</sup> mice, suggesting that c-FLIP<sub>L</sub> function can align with the function of pro-cell death proteins during embryonic development. Our data raise interesting future questions about the precise mechanism(s) employed by c-FLIP<sub>L</sub> to impact the growth of ECM-detached cells. Interestingly, c-FLIP<sub>L</sub> levels can be regulated by glutamine starvation<sup>34</sup>, and c-FLIP<sub>L</sub> can promote SGLT1-mediated glucose uptake in hepatocellular carcinoma cells<sup>35</sup>. Given these data and the fact that ECM-detachment is a profound signal to alter nutrient uptake and utilization, it is possible that the function of c-FLIP<sub>L</sub> during ECM-detachment involves alterations in cellular metabolism. Future studies aimed at better understanding the nexus between ECM-detachment, c-FLIP<sub>L</sub>, and viability will be important in order to better grasp the multi-faceted role played by c-FLIP<sub>L</sub> in cancer pathogenesis.

## Methods

**Cell culture.** MCF-10A cells (ATCC, Manassas, VA, USA) and derivatives were cultured in Dulbecco's Modified Eagle Medium/F12 (Gibco, Waltham, MA, USA) supplemented with 5% horse serum (Invitrogen), 20 ng/mL epidermal growth factor (EGF), insulin (10  $\mu$ g/mL), hydrocortisone (500  $\mu$ g/mL), cholera toxin (100 ng/mL), and 1% penicillin/streptomycin. HMEC-Human Mammary Epithelial Cells (Lonza, Basel, Switzerland) and derivatives were cultured in Mammary Epithelium Basal Medium (MEBM) (Lonza) plus MEGM Bullet-Kit and 1% penicillin/streptomycin. MDA-MB-231 cells (ATCC) and derivatives were cultured in Dulbecco's Modified Eagle's Medium with 10% fetal bovine serum (Invitrogen) and 1% penicillin/streptomycin. The small molecule inhibitors used are as follows: BYL719 (APEX-BIO, A8346), TDZD-8 (Enzo life sciences, ALX-270-354-M005) and BAY-117082 (Sigma Aldrich, B5556). Cells were grown for 24 h unless stated otherwise.

**Immunoblotting.** ECM-detached cells were harvested, washed once with cold PBS, and lysed in 1% Nonidet P-40 supplemented with protease inhibitors leupeptin (5  $\mu$ g/mL), aprotinin (1  $\mu$ g/mL), and PMSF (1 mM) and the Halt Phosphatase Inhibitor Mixture (Thermo Scientific, Waltham, MA, USA). Lysates were collected after spinning for 30 min at 4 °C at 14,000 rpm and normalized by BCA Assay (Pierce Biotechnology, Waltham, MA, USA). Normalized lysates underwent SDS-PAGE and transfer/blotting was performed as previously described<sup>16</sup>. Membranes were cut prior to incubation with primary antibodies when blotting for more than one target at a time. The following antibodies were used for western blotting: FLIP (Cell Signaling Technology, #56343), phospho-Akt (Ser473) (Cell Signaling Technology, #4060), GAPDH (Cell Signaling Technologies, #5174),  $\beta$ -tubulin (Cell Signaling Technology, #2146),  $\beta$ -Actin (Sigma-Aldrich, #A1978), phospho-I $\kappa$ B $\alpha$  (Ser32/36) (Cell Signaling Technology, 9246s), phospho-GSK-3 $\beta$  (Ser9) (Cell Signaling Technology, 5558s), and c-myc (sigma M-5546). Original, unprocessed data are available in Supplemental Figs. 5, 6.

**RNA isolation and quantitative real-time PCR.** Total RNA was isolated with RNeasy Mini Kit (Qiagen, Germantown, MD, USA). RNA (1  $\mu$ g) was reverse transcribed into cDNA using iScript Reverse Transcription Supermix Kit (Bio-Rad, Hercules, CA, USA). The relative levels of gene transcripts compared to the control gene 18S were determined by quantitative real-time PCR using SYBER Green PCR Supermix (Bio-Rad) and specific primers on a 7500 Fast Transient transfection Real Time PCR System (Applied Biosystems, Life Technologies). Amplification was performed at 95 °C for 12 min, followed by 40 cycles of 15 s at 95 °C, and 1 min at 60 °C. The fold change in gene expression was calculated as: Fold change = 2<sup>- $\Delta\Delta$ CT</sup>. The primers used are as follows: 18S



primers (F-GGCGCCCCCTCGATGCTCTTAG; R-GCTCGGGCCTGCTTTGAACACTCT), *CFLAR* primers (F-GTGGAGACCCACCTGCTCA; R-GGACACATCAGATTTATCCAAATCC), *MYC* primers (F-AGGGTC AAGTTGGACAGTGCTCA; R-TGGTCGATTTTCGGTTGTTG), *IL6* primers (F-ACATCCTCGACGGCATCT CA; R-TCACCAGGCAAGTCTCCTCA).

**Lentiviral delivery of shRNA and generation of stable cell lines.** MISSION short hairpin RNA (shRNA) constructs against *c-FLIP* (TRCN000007228 and TRCN000007230) in the puromycin-resistant pLKO.4 vector along with an empty vector control were purchased from Sigma-Aldrich. HEK293T cells were transfected with 0.5 µg target DNA along with the packaging vectors pCMV-D8.9 (0.5 µg) and pCMV-VSV-G (60 ng) using Lipofectamine 2000 and PLUS reagent (Life Technologies). Virus was collected 24- and 48-h post-transfection and filtered through a 0.45 µm filter (EMD Millipore) and used for transduction of MCF-10A cells in the presence of polybrene (8 µg/mL). Stable populations of MCF-10A cells were selected using puromycin (2 µg/mL) (Invivogen, San Diego, CA, USA).

**Retroviral mediated generation of stable cell lines.** The pBABE-Puro-based retroviral vectors encoding constitutively active HRAS<sup>G12V</sup>, EGFR, ERBB2, constitutively active P110α<sup>E545K</sup>, and myristoylated-AKT were used to generate stable cell lines. The pBABE-Puro-based retroviral vectors encoding FLIP was used to generate stable cell lines. HEK293T cells were transfected with target DNA (0.75 µg) along with the packaging vector pCLAmpho (0.75 µg) with Lipofectamine 2000 (Life Technologies). Virus was collected at 48- and 72-h post-transfection, filtered through a 0.45 µm filter (EMD Millipore), and used for transduction of MCF-10A and MDA-MB-231 cells in the presence of polybrene (8 µg/mL). Stable populations of puromycin-resistant cells were obtained using puromycin (2 µg/mL) (Invivogen, San Diego, CA, USA).

**Caspase assay.** Cells were plated at a density of 5000 cells per well on 96-well plates. Caspase activation was measured using the Caspase Glo 3/7 or Caspase 8 Assay Kit (Promega, Madison, WI, USA) according to manufacturer's instructions.

**Cell viability assay.** Cells were plated at a density of 5000 cells per well on 96-well plates. Caspase activation was measured using the Cell Titer Glo Assay Kit (Promega, Madison, WI, USA) according to manufacturer's instructions.

**Crystal violet assay.** MDA-MB-231 Cells were plated at 100,000 cells per well in poly-HEMA coated 6-well plates for 96 h. After 96 h, cells were washed and were transferred to adherent 6-well plates for 24 h. Cells were then washed with 1 × PBS and then were fixed and stained with 750 µl crystal violet solution (0.5%) for 10 min. Cells were washed with deionized water. After imaging plates, cells were destained by adding 1 ml of 10% acetic acid per well and plates were rocked for 20 min at room temperature. Samples from each well were transferred to a 96-well plate, and absorbance at 590 nm was read using a Spectramax M5 plate reader (Molecular Devices). Statistical analysis of absorbance at 590 nm was performed using two-way ANOVA.

**TCGA data analysis.** *Comparison of c-FLIP levels based on clinical attributes.* The dataset used was “Breast Invasive Carcinoma (TCGA, Firehose Legacy)”. mRNA expression data of breast cancer datasets with specific clinical attributes (ER status and PR status) was acquired. Statistical analysis on the comparison of *CFLAR* expression levels to receptor status was performed using two-way ANOVA.

*Correlation of CFLAR expression to oncogenes.* The dataset used were “Breast Invasive Carcinoma (TCGA, Firehose Legacy)” and “Lung Adenocarcinoma (TCGA, Firehose Legacy)”. Co-expression data of *CFLAR* and selected genes (HRAS, AKT1, ERBB2) was acquired from the database. Statistical analysis on the comparison of *CFLAR* expression levels to receptor status was performed using two-way ANOVA.

Received: 20 April 2021; Accepted: 30 August 2021

Published online: 20 September 2021

## References

1. Yu, J. W. & Shi, Y. FLIP and the death effector domain family. *Oncogene* **27**, 6216–6227. <https://doi.org/10.1038/onc.2008.299> (2008).
2. Ashkenazi, A. & Salvesen, G. Regulated cell death: Signaling and mechanisms. *Annu. Rev. Cell Dev. Biol.* **30**, 337–356. <https://doi.org/10.1146/annurev-cellbio-100913-013226> (2014).
3. Humphreys, L., Espona-Fiedler, M. & Longley, D. B. FLIP as a therapeutic target in cancer. *FEBS J.* **285**, 4104–4123. <https://doi.org/10.1111/febs.14523> (2018).
4. Tsuchiya, Y., Nakabayashi, O. & Nakano, H. FLIP the switch: Regulation of apoptosis and necroptosis by cFLIP. *Int. J. Mol. Sci.* **16**, 30321–30341. <https://doi.org/10.3390/ijms161226232> (2015).
5. Shirley, S. & Micheau, O. Targeting c-FLIP in cancer. *Cancer Lett.* **332**, 141–150. <https://doi.org/10.1016/j.canlet.2010.10.009> (2013).
6. Alkurdi, L. *et al.* Release of c-FLIP brake selectively sensitizes human cancer cells to TLR3-mediated apoptosis. *Cell Death Dis.* **9**, 874. <https://doi.org/10.1038/s41419-018-0850-0> (2018).
7. Chaffer, C. L. & Weinberg, R. A. A perspective on cancer cell metastasis. *Science* **331**, 1559–1564. <https://doi.org/10.1126/science.1203543> (2011).

8. Nguyen, D. X. & Massagué, J. Genetic determinants of cancer metastasis. *Nat. Rev. Genet.* **8**, 341–352. <https://doi.org/10.1038/nrg2101> (2007).
9. Buchheit, C. L., Weigel, K. J. & Schafer, Z. T. Cancer cell survival during detachment from the ECM: Multiple barriers to tumour progression. *Nat. Rev. Cancer* **14**, 632–641. <https://doi.org/10.1038/nrc3789> (2014).
10. Frisch, S. & Francis, H. Disruption of epithelial cell-matrix interactions induces apoptosis. *J. Cell Biol.* **124**, 619–626. <https://doi.org/10.1083/jcb.124.4.619> (1994).
11. Schafer, Z. T. *et al.* Antioxidant and oncogene rescue of metabolic defects caused by loss of matrix attachment. *Nature* **461**, 109–113. <https://doi.org/10.1038/nature08268> (2009).
12. Buchheit, C. L., Rayavarapu, R. R. & Schafer, Z. T. The regulation of cancer cell death and metabolism by extracellular matrix attachment. *Semin. Cell Dev. Biol.* **23**, 402–411. <https://doi.org/10.1016/j.semcdb.2012.04.007> (2012).
13. Hawk, M. A. & Schafer, Z. T. Mechanisms of redox metabolism and cancer cell survival during extracellular matrix detachment. *J. Biol. Chem.* **293**, 7531–7537. <https://doi.org/10.1074/jbc.TM117.000260> (2018).
14. Hawk, M. A. *et al.* RIPK1-mediated induction of mitophagy compromises the viability of extracellular-matrix-detached cells. *Nat. Cell Biol.* **20**, 272–284. <https://doi.org/10.1038/s41556-018-0034-2> (2018).
15. Mason, J. A., Hagel, K. R., Hawk, M. A. & Schafer, Z. T. Metabolism during ECM detachment: Achilles heel of cancer cells? *Trends Cancer* **3**, 475–481. <https://doi.org/10.1016/j.trecan.2017.04.009> (2017).
16. Davison, C. A. *et al.* Antioxidant enzymes mediate survival of breast cancer cells deprived of extracellular matrix. *Cancer Res.* **73**, 3704–3715. <https://doi.org/10.1158/0008-5472.CAN-12-2482> (2013).
17. Mason, J. A. *et al.* Oncogenic Ras differentially regulates metabolism and anoikis in extracellular matrix-detached cells. *Cell Death Differ.* **23**, 1271–1282. <https://doi.org/10.1038/cdd.2016.15> (2016).
18. Weigel, K. J. *et al.* CAF-secreted IGFBPs regulate breast cancer cell anoikis. *Mol. Cancer Res.* **12**, 855–866. <https://doi.org/10.1158/1541-7786.MCR-14-0090> (2014).
19. Mason, J. A. *et al.* SGK1 signaling promotes glucose metabolism and survival in extracellular matrix detached cells. *Cell Rep.* **34**, 108821. <https://doi.org/10.1016/j.celrep.2021.108821> (2021).
20. Kumar, B. *et al.* Normal breast-derived epithelial cells with luminal and intrinsic subtype-enriched gene expression document interindividual differences in their differentiation cascade. *Cancer Res.* **78**, 5107–5123. <https://doi.org/10.1158/0008-5472.CAN-18-0509> (2018).
21. Micheau, O., Lens, S., Gaide, O., Alevizopoulos, K. & Tschopp, J. NF- $\kappa$ B signals induce the expression of c-FLIP. *Mol. Cell. Biol.* **21**, 5299–5305. <https://doi.org/10.1128/MCB.21.16.5299-5305.2001> (2001).
22. Zhang, Q., Lenardo, M. J. & Baltimore, D. 30 Years of NF- $\kappa$ B: A blossoming of relevance to human pathobiology. *Cell* **168**, 37–57. <https://doi.org/10.1016/j.cell.2016.12.012> (2017).
23. Hoxhaj, G. & Manning, B. D. The PI3K-AKT network at the interface of oncogenic signalling and cancer metabolism. *Nat. Rev. Cancer* **20**, 74–88. <https://doi.org/10.1038/s41568-019-0216-7> (2020).
24. Park, C. Y. *et al.* Tissue-aware data integration approach for the inference of pathway interactions in metazoan organisms. *Bioinformatics* **31**, 1093–1101. <https://doi.org/10.1093/bioinformatics/btu786> (2015).
25. Dang, C. V. MYC on the path to cancer. *Cell* **149**, 22–35. <https://doi.org/10.1016/j.cell.2012.03.003> (2012).
26. Grandori, C., Cowley, S. M., James, L. P. & Eisenman, R. N. The Myc/Max/Mad network and the transcriptional control of cell behavior. *Annu. Rev. Cell Dev. Biol.* **16**, 653–699. <https://doi.org/10.1146/annurev.cellbio.16.1.653> (2000).
27. Ricci, M. S. *et al.* Direct repression of FLIP expression by c-myc is a major determinant of TRAIL sensitivity. *Mol. Cell. Biol.* **24**, 8541–8555. <https://doi.org/10.1128/MCB.24.19.8541-8555.2004> (2004).
28. Sears, R. *et al.* Multiple Ras-dependent phosphorylation pathways regulate Myc protein stability. *Genes Dev.* **14**, 2501–2514. <https://doi.org/10.1101/gad.836800> (2000).
29. Beurel, E., Grieco, S. F. & Jope, R. S. Glycogen synthase kinase-3 (GSK3): Regulation, actions, and diseases. *Pharmacol. Ther.* **148**, 114–131. <https://doi.org/10.1016/j.pharmthera.2014.11.016> (2015).
30. Debnath, J. & Brugge, J. S. Modelling glandular epithelial cancers in three-dimensional cultures. *Nat. Rev. Cancer* **5**, 675–688. <https://doi.org/10.1038/nrc1695> (2005).
31. Debnath, J. *et al.* The role of apoptosis in creating and maintaining luminal space within normal and oncogene-expressing mammary acini. *Cell* **111**, 29–40. [https://doi.org/10.1016/s0092-8674\(02\)01001-2](https://doi.org/10.1016/s0092-8674(02)01001-2) (2002).
32. Reginato, M. J. *et al.* Bim regulation of lumen formation in cultured mammary epithelial acini is targeted by oncogenes. *Mol. Cell. Biol.* **25**, 4591–4601. <https://doi.org/10.1128/mcb.25.11.4591-4601.2005> (2005).
33. Yeh, W. C. *et al.* Requirement for Casper (c-FLIP) in regulation of death receptor-induced apoptosis and embryonic development. *Immunity* **12**, 633–642. [https://doi.org/10.1016/s1074-7613\(00\)80214-9](https://doi.org/10.1016/s1074-7613(00)80214-9) (2000).
34. Mauro-Lizcano, M. & López-Rivas, A. Glutamine metabolism regulates FLIP expression and sensitivity to TRAIL in triple-negative breast cancer cells. *Cell Death Dis.* **9**, 205. <https://doi.org/10.1038/s41419-018-0263-0> (2018).
35. Lei, S. *et al.* FLIPL is critical for aerobic glycolysis in hepatocellular carcinoma. *J. Exp. Clin. Cancer Res.* **35**, 79. <https://doi.org/10.1186/s13046-016-0358-3> (2016).

## Acknowledgements

We thank Veronica Schafer and all current and past Schafer laboratory members for helpful comments, experimental assistance, and/or valuable discussion. We also thank the Siyuan Zhang lab (Notre Dame) and Xin Lu lab (Notre Dame) for technical and conceptual feedback. We thank the Sandra Van Schaeymbroeck lab (Queen's University Belfast, Belfast, UK) for sharing the c-FLIP overexpression plasmid and Harikrishna Nakshatri (Indiana University School of Medicine) for sharing the KTB cell lines. The graphic in Fig. 4G was created with Biorender.com. This work was supported by a Career Catalyst Research Grant (CCR14302768) from Susan G. Komen (to Z.T.S.), a Lee National Denim Day Research Scholar Grant (RSG-14-145-01) from the American Cancer Society (to Z.T.S.), the Coleman Foundation, the College of Science at the University of Notre Dame, and the Malanga Family Excellence Fund for Cancer Research. J.H. was supported by Mr. and Mrs. Matthew and Christine Boler as well as the Boler Family Foundation.

## Author contributions

M.A.T., J.H., K.M., I.M.M., and M.N. conducted experiments. M.A.T., J.H., K.M., I.M.M., M.N., and Z.T.S. analyzed data and interpreted results. M.A.T. and Z.T.S. wrote the manuscript with feedback from all other authors. Z.T.S. was responsible for conception/design of the project and overall study supervision.

## Competing interests

The authors declare no competing interests.

### Additional information

**Supplementary Information** The online version contains supplementary material available at <https://doi.org/10.1038/s41598-021-97715-4>.

**Correspondence** and requests for materials should be addressed to Z.T.S.

**Reprints and permissions information** is available at [www.nature.com/reprints](http://www.nature.com/reprints).

**Publisher's note** Springer Nature remains neutral with regard to jurisdictional claims in published maps and institutional affiliations.



**Open Access** This article is licensed under a Creative Commons Attribution 4.0 International License, which permits use, sharing, adaptation, distribution and reproduction in any medium or format, as long as you give appropriate credit to the original author(s) and the source, provide a link to the Creative Commons licence, and indicate if changes were made. The images or other third party material in this article are included in the article's Creative Commons licence, unless indicated otherwise in a credit line to the material. If material is not included in the article's Creative Commons licence and your intended use is not permitted by statutory regulation or exceeds the permitted use, you will need to obtain permission directly from the copyright holder. To view a copy of this licence, visit <http://creativecommons.org/licenses/by/4.0/>.

© The Author(s) 2021